Dalton Transactions

Ru–NO and Ru–NO_2 Bonding Linkage Isomerism in *cis*-$[Ru(NO)(NO_2)(bpy)_2]^{2+/+}$ Complexes – A Theoretical Insight

Journal:	*Dalton Transactions*
Manuscript ID:	DT-ART-01-2014-000016.R2
Article Type:	Paper
Date Submitted by the Author:	27-Mar-2014
Complete List of Authors:	Andriani, Karla; Universidade Federal de Santa Catarina - UFSC, Depto. de Química Caramori, Giovanni; Universidade Federal de Santa Catarina, Departamento de Química Doro, Fabio; Universidade Federal da Bahia, Departamento de Química Geral e Inorgânica Parreira, Renato; Universidade de Franca, Núcleo de Pesquisas em Ciências Exatas e Tecnológicas

Ru–NO and Ru–NO_2 Bonding Linkage Isomerism in *cis*-$[Ru(NO)(NO)(bpy)_2]^{2+/+}$ Complexes – A Theoretical Insight

Karla Furtado Andriani,*[a] Giovanni Finoto Caramori,[a] Fábio Gorzoni Doro[b,c] and Renato Luis Tame Parreira.[d]

Received (in XXX, XXX) Xth XXXXXXXXX 20XX, Accepted Xth XXXXXXXXX 20XX
DOI: 10.1039/b000000x

Ruthenium nitrosyl complexes have received considerable attention due to the fact that they are able to store, transfer and release NO in a controlled manner. It is well-known that the NO reactivity of ruthenium nitrosyl complexes can be modulated with the judicious choice of equatorial and axial ligands. In this piece of research we elucidate the nature of the Ru−NO and Ru−NO_2 bonding in a *cis*-$[Ru(NO)(NO_2)(bpy)_2]^{2+}$ complex energy decomposition (Su-Li EDA) and topological (e.g., QTAIM) and natural bond orbital analysis. It was observed that the strength of these bonds is directly correlated with the relative stability of isomers involved in nitro-nitrito and nitrosyl-isonitrosyl isomerism, as described previously by Coppens and Ooyama.

Introduction

Metal complexes with coordinated nitric oxide (NO) have received considerable attention not only in coordination chemistry but also in other fields, such as biochemistry, biology and pharmacology.[1-4] NO is able to bind with a plethora of metal centers leading to a wide variety of nitrosyl complexes (M□NO) with different geometries, coordination numbers and electronic properties.[5-14] Formally, nitric oxide can assume three oxidation states, NO^+, NO and NO^-, depending on the nature of the central atom and on the coordination environment.[12,13] Using the Enemark-Feltham $\{MNO\}^n$ notation[15] (where *n* is the number of *d*-electrons plus π* NO electrons), the formally M□NO^+, M□NO and M□NO^- cores can be represented as $\{MNO\}^6$, $\{MNO\}^7$ and $\{MNO\}^8$ (M = Ru(II) or Fe(II)), respectively. The M□NO (η^1-NO) binding mode is commonly accepted as being the ground state (GS) in the majority of metal nitrosyl complexes.[16,17] Two other linkage isomers have also been identified, the isonitrosyl M□ON (η^1-ON), MS1,[16] and a side-on (η^2-NO), MS2, (Figure 1).[16,18,19]

Fig. 1. Binding modes of nitrosyl: (i) nitrosyl - GS, (ii) isonitrosyl - MS1 and (iii) side-on - MS2.

In addition to the importance of metal nitrosyls in studies on the fundamental aspects of chemistry, such as chemical bonding and reactivity, interest in these complexes has grown in the past two decades with the discovery of the role of nitric oxide in several biological processes, for instance, in the inhibition of platelet adhesion, synaptic transmission and immune responses.[16,20-25]

[a]*Departamento de Química, Universidade Federal de Santa Catarina, Campi Universitário Trindade, 88040-900 Florianópolis – SC, Brazil. E-mail: karla.andriani@posgrad.ufsc.br; Tel: +55-48-3721-6844x239*
[b]*Departamento de Química Geral e Inorgânica, Universidade Federal da Bahia – UFBA, Salvador – BA, Brazil.* [c]*Departamento de Química, Faculdade de Filosofia, Ciências e Letras de Ribeirão Preto. Universidade de São Paulo, Av. dos Bandeirantes 3900, 14040-901, Ribeirão Preto, SP, Brazil. (present address)*
[d]*Núcleo de Pesquisas em Ciências Exatas e Tecnológicas, Universidade de Franca – UNIFRAN, Franca – SP, Brazil.*

Among the different classes of metal nitrosyls, iron or ruthenium complexes seem to be those of major importance.[10,26] Interest in iron nitrosyls can be traced to the importance of the NO interaction with heme proteins[27] and their physiological relevance.[28] In this regard, the reactivity of NO towards iron metalloporphyrins and heme proteins, such as myoglobin and their resulting NO_x (NO_x=NO, NO_2^-) derivatives, has been extensively studied.[29-31] Ruthenium nitrosyls have attracted attention as models for studying the reactivity of coordinated NO[6] as well as nitric oxide carriers.[32] The activation of $\{RuNO\}^6$, a key step in NO release, can be performed thermally (by chemical or electrochemical reduction) or photochemically.[4,32,33] Experimentally, such activation processes have been investigated by UV-Vis, EPR, IR and other techniques,[32-37] giving support to the proposed formation of intermediate species such as Ru(II)□NO^0 and Ru(III)□NO^0, respectively. The dissociation of NO from these species can be rationalized considering changes in their electronic structure upon exposure to the stimuli mentioned above. The Ru□NO interaction in $\{RuNO\}^6$ complexes, formally Ru(II)□NO^+, is dominated by strong π-back-bonding between Ru dπ orbitals and π* orbitals of NO^+, which is consistent with the thermodynamic and kinetic stability of NO with regard to dissociation.[33] The strength of the Ru□NO bond in this situation is similar to that in six-coordinated $\{FeNO\}^6$ complexes (formally Fe(II)□NO^+) with heme models in which NO dissociation is energetically unfavorable.[38] On the other hand, the NO dissociation from [Ru(III)□NO^0] species, which can also be denoted as $\{RuNO\}^6$, differs from that in the species formally known as [Ru(II)□NO^+]. In the former case the Ru□NO interaction is weak, as observed for the ferric heme NO interaction,[38] and can be attributed to a decrease in back-bonding which reduces the π-interaction.

Some ruthenium nitrosyl complexes contain polypyridine ligands such as 2,2´-bipyridine (bpy).[39] This class of complex has been shown to release NO, as observed for *cis*-$[Ru(NO)Cl(bpy)_2]^{2+}$ during photolysis in aqueous solution.[40] Silva and coworkers studied the photochemistry of a series of *cis*-$[Ru(NO)L(bpy)_2]^{3+}$ complexes (L=pyridine, 4-picoline, 4-acetylpyridine) in aqueous solution using laser flash-photolysis (λ_{irr} = 355 nm).[41] They proposed that $[Ru^{III}(NO^{\bullet})L(bpy)_2]^{3+}$ and $[Ru(ON^+)L(bpy)_2]^{3+}$ are transient species, the former being associated with NO release. Not only ruthenium nitrosyls but also nitro (Ru□NO_2) complexes have been shown to release NO.[42]

In addition to NO release, it is well known that light can trigger NO photo-induced bonding linkage isomerism,[16,32,43-46] (or metastable states), Fig. 1.[16,44-46] In most cases, these isomers have a very short life at ambient temperature. Experimentally, their photo-induced formation is investigated in the solid state and at

low temperatures.[16,17] For instance, Bitterwolf reported that photolysis in the UV (300 nm < λ_{irr} < 400 nm) and visible regions (λ_{irr}= 550 ± 35 nm) of *cis*-$[Ru(NO)Cl(bpy)_2]^{2+}$ in an ionic liquid frozen matrix at ca. 90 K provided evidence of isonitrosyl and side-on nitrosyl linkage isomers along with free NO formation.[46]

The challenge of investigating photo-induced isomerizations is enhanced when nitrito anion (NO_2^-) is present, since the two coordination modes of the monodentate ligand are nitro (η^1-NO_2) and nitrito (η^1-ONO). Complexes such as *cis*-$[Ru(NO)(NO_2)L_2]^{2+}$, where L=ammines and polypyridines ligands, may display not only nitrosyl-isonitrosyl isomerism but also nitro-nitrito isomerism.[47] These processes can take place through intramolecular oxygen transfer.

After oxygen transfer, the remaining NO group can still exhibit nitrosyl-isonitrosyl isomerism.[16,47-52] Kovalevsky and coworkers[53] showed, via crystallographic and IR analyses, that at low temperatures (90 K) intramolecular oxygen transfer occurs from the nitro to the nitrosyl group. At 200 K, only the isomer containing the nitrito ligand was observed (Fig. 2). The results of their mechanistic investigation indicated that the oxygen transfer proceeds via a side-on bound transition state, explaining the stability of the *cis*-$[Ru(NO)(ONO)(bpy)_2]^{2+}$ complex and the non-existence of *cis*-$[Ru(ON)(NO_2)(bpy)_2]^{2+}$. Coppens and coworkers[16] showed that the metastable states of ruthenium nitrosyl complexes such as *cis*-$[Ru(NO)(NO_2)(bpy)_2](PF_6)_2$ are not electronically excited states, but rather linkage isomers, as also discussed by Sizova.[44,48]

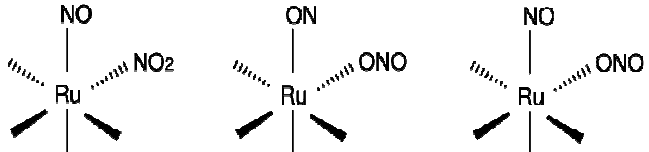

Fig. 2. Nitro bonding linkage isomerism: (i) and (iii) GS and (ii) MS1 binding modes of nitrosyl.

Electronic structure calculations, especially those based on DFT methods, are widely used in investigations on the chemistry of nitrosyl complexes, providing information on the geometries and the electronic structure of {M□NO} cores and aiding the assignment of the bands on electronic spectra, stretching frequencies and, frontier orbitals or even the evaluation of the excited states of ground or photoinduced metastable states, electronic transitions and spin density distributions.[18,31,38,44,47,53-64] For instance, DFT calculations have been successfully employed to investigate the occurrence of Fe(II)□NO^+ and Fe(III)□NO electronic states in ferric heme nitrosyls.[38] They have also been employed to differentiate local and global minima of the Cu(I)□NO bonding modes (end-on or side-on) in cooper nitrito reductase.[18] Kaim and coworkers[62] have used DFT calculations to reproduce structural features and to provide stretching frequencies and spin-density representations of complexes containing redox-active metals and two different non-innocent ligands, L_1□M□L_2, specifically complexes such as $[Ru^k(NO^m)(Q^n)(terpy)]^{2+}$, where k = 2+ or 3+; m = 0, + or -; and Q^n = quinone (n = 0), semiquinone (n=1-), or 2-anilidophenolato (n=2-). Kaim and Lahiri[65] explore the alternatives for the electronic structure of {RuNO} cores (Ru^{III}□NO^+ ={$RuNO$}^{5} Ru^{II}□NO^+ = {$RuNO$}^{6}, Ru^{II}□$NO^·$ = {$RuNO$}^{7}, Ru^{II}□NO^- = {$RuNO$}^{8}) in ruthenium nitrosyl complexes, $[Ru(NO)L_n]$, containing non-innocent ligands. Using the Enemark-Feltham notation in conjunction with experimental and DFT data they present a concise description of the oxidation state. Based on papers discussing {RuNO}^{x} [31,38,62,66-68] or {FeNO}^{x} [31,38] configurations, the logical assumption, which is supported by experiments and DFT calculations,[31,38,62,65-68] is that in {RuNO}^{6} or {FeNO}^{6} interactions the role of π back-donation from occupied d_π orbitals to empty π^* orbitals of NO^+ is crucial, or even that {RuNO}^{7} cores present an enhanced covalent character. However, most authors have not focused on the physical origin of such interactions. The following questions still need to be addressed: (i) What is the contribution of exchange and charge transfer to the well-known π-back-donation in {RuNO}^{6} and {FeNO}^{6} systems? (ii) To what extent are electrostatic and dispersion contributions present in the {RuNO}^{6} and {RuNO}^{7} interactions? (iii) How strong are the electrostatic and covalent characters in {RuNO}^{6} and {RuNO}^{7} interactions and are these interactions affected by the presence of other non-innocent ligands? The aim of the study reported herein was to address these questions by presenting a robust and elegant theoretical approach in which the interaction energy can be decomposed into physical meaningful terms. This will help to improve our understanding and provide further information regarding the nature of the chemical interactions involved, taking into account the electronic effects associated with the vicinity. This approach is called energy decomposition analysis (EDA). In this study, the Su-Li EDA[69] was employed to investigate the nature of {RuNO}^{6}, Ru(II)□NO^+ and Ru(II)□ON^+ and also of {RuNO}^{7}, Ru(II)□NO^0 and Ru(II)□ON^0 as well as Ru(II)□NO_2^- and Ru(II)□ONO^- bonding in *cis*-$[Ru(NO)(NO_2)(bpy)_2]^{2+}$ complexes. The objective is to enhance our understanding of the main processes that govern the chemical behavior of metal-ligand bonding, particularly in relation to nitrosyl-isonitrosyl and nitro-nitrito bonding linkage isomerism. Additional insights into the nature of the Ru−NO and Ru−NO_2 bonding are provided by means of QTAIM (Quantum Theory of Atoms in Molecules)[70-74] and NBO (Natural Bond Orbitals)[75] analyses. The findings reported herein allow a better comprehension of the experimental results obtained by Coppens and coworkers,[16] explaining why the *cis*-$[Ru(ON)(NO_2)(bpy)_2]^{2+}$ isomer has not yet been observed.

Methods

All calculations were performed with ORCA2.8[76] GAMESS01.10.10[77] and GAUSSIAN03[78] program packages. Geometry optimizations, harmonic frequencies and single point calculations for all complexes were carried out using the BP86,[79-81] GGA functional. The triple ζ – quality Ahlrich's basis set Def2-TZVPP,[82] with two sets of polarization functions, was used for ruthenium, nitrogen, oxygen and hydrogen atoms. In addition, auxiliary basis sets were used to expand the electron density in the resolution of identity (RI) approach, and Def2-TZVPP and Def2-TZVPP/J and ECP[83] were employed for the ruthenium ion. Scalar relativistic effects were considered for the ruthenium ion using the zero-order regular approximation (ZORA).[84-86] All structures reported herein were verified as local energy minima on the potential energy surface.

The nature of Ru−NO and Ru−NO_2 bonds was analyzed different methodologies, including energy decomposition analysis (Su-Li EDA[69]), which was employed to characterize the physical nature of the Ru(II)□NO, Ru(II)□ON, Ru(II)□NO_2 and Ru(II)□ONO bonds in the {RuNO}^{6} (**1a-3a**) and {RuNO}^{7} (**1b-3b**) cores, considering the fragmentation scheme presented in Tables 2 and 3.

Su-Li EDA analysis is an important tool used to investigate the nature of chemical bonding, which is rooted in the prototypical EDA methods of Kitaura and Morokuma (KM),[87,88] Ziegler and Rauk (ZR)[89] and Hayes and Stone (HS)[90]; however, it includes modifications and extensions of these methods. For a set of

orthonormal molecular Hartree-Fock spin orbitals, the Hartree-Fock energy, E^{HF}, can be written in terms of orbital energy integrals, Eq. (1), in which *i* and *j* run over occupied spin orbitals, the one-electron, two-electron, Coulomb and exchange integrals, are given by h_i, $\langle ii|jj\rangle$, and $\langle ij|ij\rangle$, respectively, and E^{nuc} represents the nuclear repulsion energy. For a molecule X comprised of A fragments the total HF interaction energy, $\Delta E^{\text{int}}_{\text{HF}}$, can be written as Eq.(2), in which $|\Phi_X\rangle$ and $|\Phi_A\rangle$ represent the single-determinant wavefunctions for the molecule and fragment, respectively.

$$E^{HF} = \sum_{i}^{\alpha,\beta} h_i + \frac{1}{2}\sum_{i}^{\alpha,\beta}\sum_{j}^{\alpha,\beta}\langle ii|jj\rangle - \frac{1}{2}\sum_{i}^{\alpha}\sum_{j}^{\alpha}\langle ij|ij\rangle - \frac{1}{2}\sum_{i}^{\beta}\sum_{j}^{\beta}\langle ij|ij\rangle + E^{nuc} \quad (1)$$

$$\Delta E^{\text{int}}_{\text{HF}} = \langle \Phi_X | H_X | \Phi_X \rangle - \sum_A \langle \Phi_A | H_A | \Phi_A \rangle \quad (2)$$

In the Su-Li EDA, the interaction energy, Eq. (2), is decomposed into a number of physically meaningful components, such as the electrostatic, exchange, repulsion and polarization components, as in Eq. (3):

$$\Delta E^{\text{int}}_{\text{HF}} = \Delta E^{\text{ele}} + \Delta E^{\text{exe}} + \Delta E^{\text{rep}} + \Delta E^{\text{pol}} \quad (3)$$

The electrostatic term, ΔE^{ele}, for RHF cases is the same as in the Kitaura-Morokuma EDA, but applicable to molecules comprised of many fragments. Physically, ΔE^{ele} corresponds to the interaction energy involved in the process of bringing the fragments into the final configuration of the molecule, while keeping the wavefunctions constant as in isolated fragments. In the Su-Li EDA, the exchange-repulsion energies consist of both exchange, ΔE^{exe}, and repulsion, ΔE^{rep}, components. At the HF level, the former is given in terms of exchange integrals involving r_{ij}^{-1}, while the latter involves integrals over the kinetic energy and electron-nuclear Coulomb operators. According to Hayes and Stone, ΔE^{rep} represents a mixture of electron–electron repulsion and electron-nuclear and electron kinetic energy effects. In RHF cases, the sum of the exchange and repulsion components in Su-Li EDA corresponds to the exchange-repulsion term in the Kitaura-Morokuma EDA. The polarization component, ΔE^{pol}, involves interactions between occupied and unoccupied orbitals within the same fragment and also interactions between occupied orbitals from one fragment and unoccupied orbitals of the other fragments and vice versa. Therefore, the polarization term in the Su-Li EDA includes both the polarization, charge transfer and mixing terms of the Kitaura-Morokuma scheme.[87,88] The electrostatic, repulsion and exchange terms are isolated according to the Hayes and Stone method.

Since the Su-Li EDA is based on spin-orbitals, it can be used to deal with both closed- and open-shell systems described by RHF, ROHF, or UHF wavefunctions. The dispersion energy, Eq.(4), is derived through correlation methods such as MP2 or CCSD(T). It is important to emphasize that the dispersion term in the Su-Li EDA is, in fact, the MP2 correction to the Hartree-Fock interaction energy, including higher-order corrections with the electrostatic, exchange-repulsion and polarization energies.

$$\Delta E_{\text{MP2}} = \Delta E^{\text{ele}} + \Delta E^{\text{ex}} + \Delta E^{\text{rep}} + \Delta E^{\text{pol}} + \Delta E^{\text{disp}} \quad (4)$$

Similarly to the HF method, Eq. (1) can be written in terms of a single-determinant wavefunction, Ψ_i, formed by a set of orthonormal Kohn-Sham orbitals (KS), Eq.(5), in which h_i and $\langle ii|jj\rangle$ are the one and two-electron integrals and E^{nuc} is the nuclear repulsion energy, E^{nuc}, $E_x[\rho^\alpha,\rho^\beta]$ and $E_c[\rho^\alpha,\rho^\beta]$ are the exchange and correlation functionals, and ρ^α and ρ^β are spin-alpha and spin-beta electron densities.

$$E^{KS} = \sum_{i}^{\alpha,\beta} h_i + \frac{1}{2}\sum_{i}^{\alpha,\beta}\sum_{j}^{\alpha,\beta}\langle ii|jj\rangle + E_x[\rho^\alpha,\rho^\beta] + E_c[\rho^\alpha,\rho^\beta] + E^{nuc} \quad (5)$$

As in the HF method, for a molecule *X* comprised of *A* fragments, the total KS interaction energy is defined according to Eq.(6). In the DFT version of the Su-Li EDA implemented in GAMESS-US, the total interaction energy, $\Delta E^{\text{int}}_{\text{KS}}$, is decomposed into electrostatic, ΔE^{ele}, exchange, ΔE^{ex}, repulsion, ΔE^{rep}, polarization, ΔE^{pol}, and dispersion, ΔE^{disp}, components, Eq.(7), which are dependent on the exchange and correlation functionals employed. The Boys and Bernardi[91] counterpoise method is also implemented in the Su-Li EDA approach to correcting the basis set superposition error (BSSE). Further details can be found in Su and Li's paper.[69]

$$\Delta E^{\text{KS}} = E_X^{KS} - \sum_A E_A^{KS} \quad (6)$$

$$\Delta E^{\text{int}}_{\text{KS}} = \Delta E^{\text{ele}} + \Delta E^{\text{ex}} + \Delta E^{\text{rep}} + \Delta E^{\text{pol}} + \Delta E^{\text{disp}} \quad (7)$$

The Su-Li EDA analysis was performed in the GAMESS[77] package using the Zhao-Truhlar hybrid functional M06[92,93] and Ahlrich's Def2-SVP basis sets.[82] Additional insights into the nature of the Ru(II)□NO, Ru(II)□ON, Ru(II)□NO_2, and Ru(II)□ONO bonding in {RuNO}^{6} (**1a-3a**) and {Ru□NO}^{7} (**1b-3b**) cores were obtained by means of QTAIM[70-74] and NBO[75] analyses. The QTAIM analysis was carried out using the AIMALL12.11.09[94] and Multiwfn2.3[95] softwares.

Results and Discussion

Ground and metastable state structures of *cis*-[Ru(NO)(NO$_2$)(bpy)$_2$]$^{2+/+}$ complex

The optimized structures of {RuNO}^{6} in the GS (**1a** and **3a**) and MS (**2a**) states as well as their one-electron reduced analogues {RuNO}^{7} (**1b-3b**) are shown in Fig. 3. Both isomeric forms of coordinated NO exhibit pseudo-octahedral structures, belonging to the C_1 point group. The geometric parameters are presented in Table S1 (supporting information) and, as observed for Ru□N/O(1), N(1)□O(1) and Ru□N/O(2), the bond lengths are in close agreement with theoretical and experimental data available in the literature.[16,49] The ONO$^-$ binding mode of the NO_2^- group in the *cis* position to NO in the GS of {RuNO}^{6} complexes is unusual.[49,96] In complex **3a**, the Ru□N(1)□O(1) bond angle is 175^o, which is in good agreement with the values observed experimentally for [Ru(TPA)(ONO)(NO)](PF$_6$)$_2$ (176^o).[96] The DFT analysis at the BP86/TZVP level of theory performed for different isomers of the TPA (tris(2-pyridylmethyl)amine) complex showed that the NO_2^- and ONO$^-$ groups in the *cis* position to NO lead to Ru□N(1)□O(1) bond angles of 179^o and 175^o, respectively. This small decrease was also observed upon nitro to nitrito isomerization in complexes **1a** and **3a** and it did not influence the Ru□N(1) bond length (1.732

Å and 1.737 Å, respectively). For complexes **1a, 2a** and **3a** the bond angles for Ru□N(1)□O(1) and Ru□O(1)□N(1) ranged from 175.62° to 177.62°, which is consistent with the nitrosonium character of the NO^+ ligand. Nitro to nitrito isomerization (complexes **1a** and **3a**) only slightly diminishes the Ru□N(1)□O(1) bond angles and does not influence the Ru□N(1) bond length (1.732 Å and 1.737 Å, respectively). In these isomers the individual bonds of the NO_2^- ligand can be differentiated by their bond lengths, values for the N(2)□O(2) and N(2)□O(3) for nitro being 1.226 Å and 1.232 Å while for nitrito they are 1.450 Å and 1.172 Å, respectively (Table S1). Upon NO isomerization, no significant changes were observed in the Ru□O(2) bond length for the nitrito ligand between isonitrosyl (**2a**) and nitrosyl (**3a**). This behavior is consistent with the less pronounced electronic interaction of the ligand in the *cis* compared to the *trans* position. N(1)□O(1) and O(1)□N(1) are essentially the same in these isomers.

Investigations on the effect of the addition of one electron to the NO group in a series of isomers are scarce. This changes not only the electronic properties of $\{RuNO\}^6$ complexes but also their structural features and reactivity.[96-98] The monoelectronic reduction of $\{RuNO\}^6$ to $\{RuNO\}^7$ species (complexes **1b, 2b** and **3b)** results in changes in the geometric parameters. The Ru□N(1)□O(1) and Ru□O(1)□N(1) bond angles change from the almost linear to the angular bent form, as shown in Fig. 3 and Table S1. This bending can be interpreted as Jahn-Teller splitting due to the breaking of the degeneracy of π* orbitals LUMO and LUMO +1 after the addition of one electron, due to the lowering of the symmetry and spin-orbit interaction, as previously observed by Lahiri and coworkers.[67] Caramori and Frenking[97] have also investigated the variations in the EDA components on changing the Ru□N□O angle from the bent to the linear form in the $\{RuNO\}^7$ core of *trans*-$[Ru^{II}(NH_3)_4(Cl)NO]^{+1}$ complexes. They observed not only a considerable increase in the electrostatic and orbital terms but also a decrease in the Pauli repulsion, indicating that if only the Pauli repulsion is taken into account a false impression is created, because it decreases as the Ru□N(1)□O(1) angle increases, while, at the same time, a fast increase in the electrostatic component is observed. The above-mentioned authors also observed that the total interaction energy profile follows a trend similar to that of the orbital interaction values, indicating that the bending of the Ru□N(1)□O(1) angle minimizes the electrostatic repulsion and also provides a conformation where the orbital interactions are maximized.

Both Ru□N(1) and Ru□O(1) bond distances are lengthened and are thus weaker compared to those in $\{RuNO\}^6$. This lengthening is marked in *cis*-$[Ru(ON)(ONO)(bpy)_2]^+$, in which Ru□O(1) increases by 0.211 Å. Figure 3 also shows that the N(1)□O(1) and O(1)□N(1) bond lengths are slightly lengthened in comparison with their non-reduced forms. The nitro group is recognized as a good σ-donor which can also exhibit π-acceptor properties, while the linearly coordinated nitrosyl ligand (NO^+) is a strong π-acceptor but weak σ-donor. Its reduced bent form (NO^0) is a better σ-donor, but may also participate in some π-back-bonding. The *trans* influence of NO is especially important in six-coordinate ferrous heme-nitrosyls, which have been studied in detail.[100,101] Not only NO but also nitrito are known to exhibit structural *trans*-effects (STE).[102] Since the monoelectronic reduction of $\{RuNO\}^6$ as well as the different binding modes of the NO and NO_2^- groups are expected to modify their σ-donor and π-acceptor properties, the Ru□N(4) and Ru□N(5) bond length values allow some conjecture on the *trans* effect of such groups in different situations. It should be noted that Ru□N_{bpy} distances in the bidentate bpy ligand may be less prone to variation and thus only slight differences should also be expected. With the exception of **2a** and **2b,** in which isonitrosyl is present, the bonds of Ru□N_{bpy} *trans* to NO_2^- or NO are consistently longer than the other Ru□N_{bpy} bonds that are *not* in the *trans* position to these groups, as observed experimentally and theoretically.[16]

In $\{RuNO\}^6$ complexes the Ru□N(3) and Ru□N(6) (not *trans* to NO_2^- nor NO) bond lengths are almost the same and they range from 2.096 to 2.058 Å with an average value of 2.073±0.009 Å (Table S1). In contrast, bond lengths of 2.144 and 2.116 Å were observed for Ru□N(5) in complexes **1a** and **3a**, respectively. This is in agreement with the strong π-acid character of linear coordinated NO. The NO_2^- group (N- or O-bonded) seems to exert a relatively small *trans* effect on these complexes since Ru□N(4) bonds (2.127 and 2.102 Å, respectively) are only slightly longer than the average bond length observed for Ru□N(3) and Ru□N(6). According to these values, the nitrito group seems to exert a smaller *trans* effect than the nitro group. Notably, in **2a**, where both NO and NO_2^- are O-bonded, Ru□N(4) (2.089 Å) and Ru□N(5) (2.040 Å) are shortened in relation to **1a** and **3a** and are essentially within the range of the Ru□N(3) and Ru□N(6) bond lengths, suggesting that this linkage isomer may present the least favorable character for the *trans* effect. In agreement with the angular bent mode observed in complexes **1b** and **3b,** as a result of the addition of one electron to NO, the Ru□N(5) bonds are lengthened to 2.154 Å and 2.161 Å, respectively, indicating a stronger *trans* effect. In complex **2b** all Ru□N_{bpy} bond lengths are fairly close, as observed for **2a**. The bond angles exhibit different behaviors; for the nitro isomer they are close to 115.95° for **1a** prior to the reduction and 117.31° for **1b** after reduction, while the nitrito isomer presents the opposite behavior, the bond angle decreasing with the reduction from 116.37° to 115.63° for isomers **3a** and **2b**, respectively.

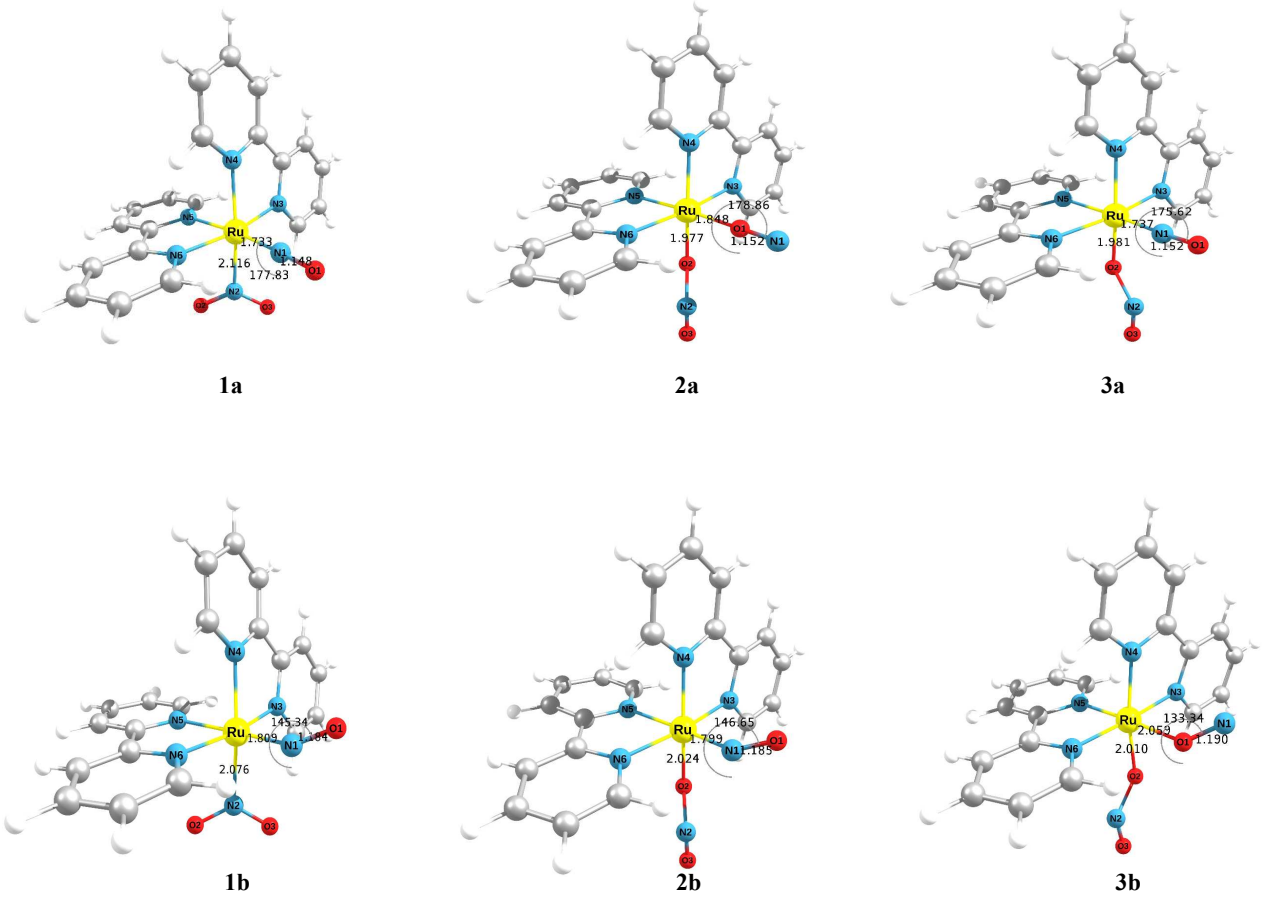

Fig. 3. Representation of the reduction of $\{RuNO\}^6$ core species (**1a-3a**) generating the reduced $\{RuNO\}^7$ species (**1b-3b**) for nitrito Z forms. The atom labels are given in the figure.

The stretching frequencies of the NO group, ν(NO), (stretching mode, Table S1) for **1a-3a** are consistent with those observed experimentally. After reduction, the ν(NO) values shift to lower wavenumbers on going to **1b-3b**, in agreement with the increase in the N(1)–O(1) and O(1)–N(1) bond lengths and the nitrosyl character of NO. Similar behavior was observed for the NO_2^- group and the $\nu_a(NO_2^-)$ values shift to lower wavenumbers after reduction. Before discussing the nature of the bonding for the above mentioned isomers, it is important to note that the nitrito-ligand can present two different configurations, known as forms *U* and *Z*. It was observed that on passing from the U-form to Z-form in isomers **2a** and **3a**, a slight energy destabilization takes place, as previously observed by Kovalevsky and Coppens.[53] This destabilization is observed not only prior to (Figure 4a) but also after the monoelectronic reduction, in isomers **2b** and **3b** (Figure 4b). Prior to the reduction the U-shaped nitrito form **3aU** is energetically slightly more stable than in the GS, **1a** (Figure 4a).

However, this behavior is not observed after the monoelectronic reduction. In fact, **3bU** is less stable than **1b** by 2.3 kcal mol^{-1} (Figure 4b). The difference in energy between the U and Z forms is quite similar for the isomers **2a** (NO bonded as isonitrosyl) and **3a** (NO bonded as nitrosyl). In agreement with Kovalevsky and Coppens,[53] the energy level is calculated as 43.1 kcal mol^{-1} prior to the reduction and 28.2 kcal mol^{-1} after the NO reduction (Figures 4a and 4b).

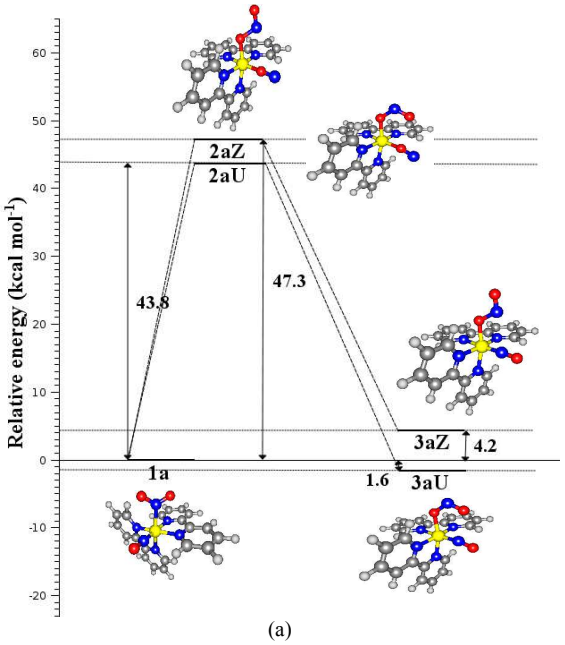

(a)

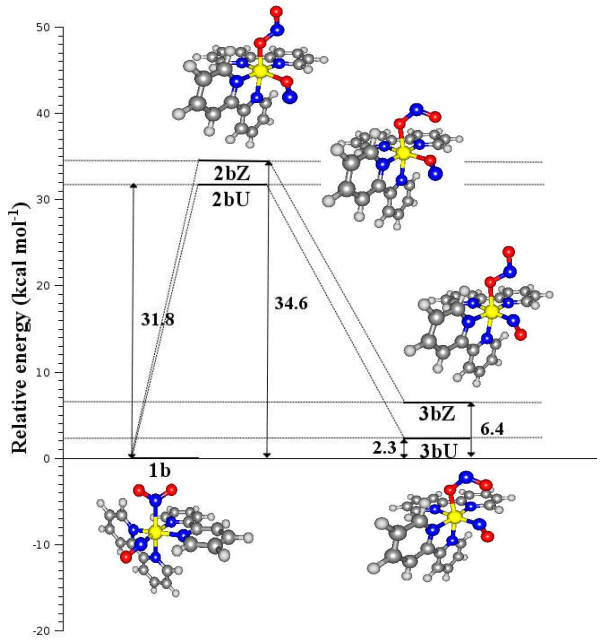

Fig. 4. Calculated energy profile (kcal mol^{-1}) for linkage isomers relative to the ground state (GS) structure **1a**. The energy levels are computed taking into account the changes in the nitrito-ligand configuration (U-form and Z-form), prior to (a) **1a-3a** and after (b) **1b-3b** the monoelectronic reduction, considering BP86/Def2-TZVPP as the level of theory.

NBO and QTAIM Analyses

For the sake of clarity and simplicity, the values presented and discussed in this section are related to the Z-form of the nitrito ligand configuration, since similar trends were observed for the forms Z and U. For instance, they present similar bond lengths, indicating that the Ru□N(1)O(1) bond distance in **3aU** (1.773 Å) is larger than in **3aZ** (1.737 Å). Similarly, the Ru□O(1)N(1) bond distance in **2aU** (1.879 Å) is larger than in **2aZ** (1.848 Å). On the other hand, the Ru□O(2)N(2)O(3) bond distances are slightly larger in the U form than in the Z form (**2aU** (2.035 Å), **2aZ** (1.977 Å), **3aU** (2.042 Å), and **3aZ** (1.928 Å)).

The bond order values (Table 1) indicate that the NO group binds more strongly in the GS than in the MS1 state. For instance, the bond order values for {RuNO}^{6} in the GS are twice those in the MS1 state, in which Ru–N(1) exhibits something between a single and double bond character, while Ru–O(1) presents a donor-acceptor electronic character. After the addition of one electron to {RuNO}^{6} the reduction in the Ru–N(1) and Ru–O(1) bond orders is accompanied by an increase in the bond lengths and a decrease in the vibrational frequencies, ν(NO), suggesting that the NO group has a nitrosyl character.

Table 1. Wiberg bond order for **1a-3b** isomers at M06/Def2-SVP level of theory.

Bond	**1a**	**1b**	**2a**	**2b**	**3a**	**3b**
Ru–N(1)	1.380	1.019			1.371	1.056
Ru□O(1)			0.680	0.390		
N1□O(1)	1.978	1.800			1.958	1.775
O(1)□N(1)			1.956	1.767		
Ru□N(2)	0.477	0.502				
Ru□O(2)			0.541	0.476	0.535	0.469
N(2)□O(2)	1.566	1.519				
O(2)□N(2)			1.018	1.127	1.022	1.128
N(2)□O(3)	1.541	1.531	1.972	1.866	1.973	1.805
Ru□N(3)	0.471	0.412	0.430	0.468	0.430	0.414
Ru□N(4)	0.331	0.301	0.387	0.545	0.379	0.296
Ru□N(5)	0.361	0.391	0.502	0.448	0.363	0.415
Ru□N(6)	0.433	0.428	0.436	0.435	0.435	0.452

As also observed in Table 1, the Ru–O(1) bond order most affected is that for **2b**, which decreases by almost 42% when compared with the oxidized form **2a**, while the decrease in the bond orders upon reduction for **1a** and **3a** ranges from 22% to 26%. The decrease in the bond order and increase in the Ru–O(1) bond length for complex **2b** suggests that in this complex the $[ON]^0 \leftrightarrow [Ru(ONO)(bpy)_2]^+$ interaction has a lesser effect on the total interaction energy when compared with $[ON]^0 \leftrightarrow [Ru(NO_2)(bpy)_2]^+$ and $[NO]^0 \leftrightarrow [Ru(NO_2)(bpy)_2]^+$ for **3b** and **1b,** respectively**.**

The N(1)–O(1) bonds present similar bond orders prior to and after the monoelectronic reduction. Due to the addition of one electron to the NO π* orbital the bond orders become small after the monoelectronic reduction.

The Ru–NO_2 and Ru–ONO bond orders are quite similar, but their values are dependent on the reduction of the nitrosyl group (Table 1). The Ru–NO_2 bond orders increase with the nitrosyl reduction, while the Ru–ONO bond orders decrease. This behavior was confirmed by the Su-Li EDA. The similarity between the Ru–ONO bond orders in **2a** and **3a** (0.541 and 0.535, respectively) indicate that η^1-NO to η^1-ON isomerization does not have any influence on the $[ONO]^- \leftrightarrow [Ru(NO)(bpy)_2]^{3+}$ interaction. In contrast to Ru–NO_2, after reduction the Ru–ONO bond orders for **2b** and **3b** (0.476 and 0.469, respectively) are lower than those for **2a** and **3a**, which suggests that after the reduction the Ru–ONO bond becomes weaker than the Ru–NO_2 bond.

The individual bonds of the nitro and nitrito groups can be differentiated by their bond lengths and bond orders. The nitro group presents a formal bond order of 1.5 for N(2)–O(2) and N(2)–O(3), confirming the resonance between these bonds. On the other hand, for the nitrito group asymmetry of the N–O bonds was observed. The N(2)–O(3) bond has a typical double bond character, while the N(2)–O(2) bond presents a single bond character. These results are in agreement with those reported for Cu nitrito complexes with the tris(pyrazolyl)methane ligand (L1′), [Cu(L1)(ONO)(NO_2)].[103]

The bond orders for the bonding of the ruthenium ion with the bipyridine nitrogens have the same nature and are of similar magnitude to those observed for the Ru–N(3) and Ru–N(6) bond orders in **1a** (0.471 and 0.430), **2a** (0.430 and 0.436**)** and **3a** (0.433 and 0.435). The lower bond order values for Ru–N(5) (*trans* to NO) in **1a** and **3a** compared to **2a** are in agreement with a stronger *trans* influence of nitrosyl on the isonitrosyl Ru−ON binding mode of NO, which is consistent with the results observed and discussed in the previous section. After the reduction there is a decrease in the Ru–N(3) (0.412 for **1b** and 0.414 for **3b**) and Ru–N(4) (0.301 for **1b** and 0.296 for **3b**) and an increase in the Ru–N(5) (0.391 for **1b** and 0.415 for **3b**) and Ru–N(6) (0.428 for **1b** and 0.452 for **3b**) bond orders for isomers **1b** and **3b**, in agreement with the lengthening of the Ru–N(3) and Ru–N(4) bonds and shortening of the Ru–N(5) and Ru–N(6)

bonds after reduction. However, the opposite behavior was observed for complex **2b,** in which an increase in the Ru–N(3) (0.468) and Ru–N(4) (0.545) and a decrease of Ru–N(5) (0.448) and Ru–N(6) (0.435) bond orders was observed.

The calculation of the atomic charge distribution (Table S2) gave positive partial charges for Ru in compounds **1a** (+0.695 e), **2a** (+0.867 e) and **3a** (+0.816 e), while NO_2^- in **1a** and the ONO groups in **2a** and **3a** carry negative partial charges, -0.338 e, -0.465 e and -0.442 e, respectively. On the other hand, the NO^+ and ON^+ groups carry positive charges only. These trends in the charge distribution are in full agreement with the Su-Li EDA analysis, which showed that prior to the reduction the Ru–NO_2 and Ru–ONO bonds have a strongly attractive electrostatic contribution, $\bullet E^{ele}$, while the Ru–NO bonds exhibit repulsive electrostatic contributions (Table 2). After the monoelectronic reduction of the NO^+ group, the charge distribution is somewhat different. The NO^0 groups present negative charges, but close to zero (**1b** (-0.022 e), **2b** (-0.066 e) and **3b** (-0.043 e)), while the Ru atoms carry positives charges, but lower than those prior to the reduction (**1b** (+0.555 e), **2b** (+0.707 e), and **3b** (+0.676 e)). On the other hand, the partial charges of the ONO^- and NO_2^- groups are still more negative than those observed prior to the reduction (Table S2), indicating that the electron-donicity of the nitrito group changes with the binding mode. This result was reinforced by the Su-Li EDA (Table 3) which indicated that the electrostatic contribution in the $\{RuNO\}^7$ and $\{RuON\}^7$ bonds become attractive in comparison with $\{RuNO\}^6$ while the electrostatic stabilization of Ru–ONO^- and Ru–NO_2^- is reduced after the monoelectronic reduction. The polarization and hybridizations of the NBOs given in Table S3 indicate that prior to the monoelectronic reduction the Ru−NO bond is polarized toward the nitrosyl ligand in **1a** while complex **3a** shows the opposite behavior, in which the Ru−NO bond is polarized toward the ruthenium center. The nature of the bonding of the isonitrosyl group in **2a** is clearly different from that of the nitrosyl group, and an effect on the polarization coefficients was not observed, while the isonitrosyl and ruthenium groups presented similar values for the polarization coefficients (45.90% and 54.10%, respectively). However, in comparison with **1a**, these values are high, which can be attributed to the coordination of the ONO group, since it donates less electron density to the ruthenium atom. Table S3 also shows the NBO hybridizations after the monoelectronic reduction $\{RuNO\}^7$. According to the results, the bonding is polarized towards the ruthenium atoms and comprises the Ru−NO and Ru−ON bonds resulting from the overlap between the *d* orbital of Ru with a *p* orbital located at the N or O atoms.

For the nitro and nitrito groups, the polarization tendency is the same prior to and after the reduction, as shown in Tables S2 and S3, changing to nitro in complex **1** and to nitrito in complexes **2** and **3**. To balance the charge distribution/flux of the $\{RuNO\}^{6/7}$ cores the behavior of the polarization for the Ru−NO_2 and Ru−ONO bonds is the opposite to that of the Ru−NO and Ru−ON bonds. After the monoelectronic reduction a decrease in the polarization was observed for the ruthenium centers in **1b** and **2b** and an increase was noted in the case of **3b**, which is in agreement with the calculated atomic charge distributions (Table S2), while an increase in the polarization coefficients was observed for the nitro and nitrito groups in **1b** and **2b** and a decrease was noted for **3b**.

The covalent character of Ru−NO, Ru−ON and Ru−NO_2 bonds was verified by the QTAIM analysis results (Table S4, supporting information). The covalent character of a bond is characterized by a negative Laplacian value at the critical point of the bond ($\bullet^2\rho_b < 0$) while closed-shell interactions have positive values of $\bullet^2\rho_b$. The results suggest that all bonds have closed-shell interactions, where the Ru−NO and Ru−ON bonds have a stronger closed-shell character than the Ru−NO_2 and Ru−ONO bonds. Complex **1a** had a higher $\bullet^2\rho_b$ (1.148 a.u.) than **2a** and **3a** (1.010 and 1.134 a.u., respectively), which suggests that the Ru−NO bond in the $\{RuNO\}^6$ interaction in **1a** and **3a** has a more covalent character than the Ru−ON bond in the $\{RuON\}^6$ interaction in **2a**, as also confirmed by the Su-Li EDA results (Table 2) which showed a more stabilizing polarization component for Ru−NO bonds than for Ru−ON bonds. After the monoelectronic reduction, a decrease in the Laplacian value was observed, suggesting that the covalent character of the $\{RuNO\}^7$ and $\{RuON\}^7$ interactions is reduced in comparison with the $\{RuNO\}^6$ and $\{RuON\}^6$ interactions, which is also in agreement with the orbital polarization observed in the Su-Li EDA (Table 2 and 3). The Laplacian values for the Ru−NO_2 and Ru−ONO bonds showed different behaviors. Prior to the reduction complex **2a** had a higher $\bullet^2\rho_b$ value (0.508) than **1a** and **3a** (0.298 and 0.486 a.u., respectively). However, after the monoelectronic reduction, a decrease in the covalent character of the Ru−ONO bonds was observed in complexes **2b** and **3b**, while an increase occurred for complex **1b**, from 0.298 to 0.366 a.u.

Bonding Energy Decomposition Analysis

Nitrosyl↔Isonitrosyl isomerism of $\{RuNO\}^6$ cores.

The Su-Li EDA analysis was carried out considering $[NO]^+$, $[ON]^+$, $[Ru(NO_2)(bpy)_2]^+$ and $[Ru(ONO)(bpy)_2]^+$ as the interacting fragments (Table 2). To shed light on how nitrosyl bonding linkage isomerism affects nitro↔nitrito isomerism and vice versa, the $[NO_2]^-$ and $[ONO]^-$ interaction with $[Ru(NO)(bpy)_2]^{3+}$ and $[Ru(ON)(bpy)_2]^{3+}$ was also evaluated and the results are reported in Table 2.

In this context, it is important to clarify the physical differences between the total bonding energy, $\bullet E^{int}$, and the bond dissociation energy, *-De*. The total interaction energy in the Su-Li EDA, $\bullet E^{int}$, corresponds to the instantaneous interaction between two or more interacting fragments, which can be evaluated at the Hartree-Fock, HF, or DFT levels of theory, as described in the methodology section. One way to estimate the bond dissociation energy is by computing the total preparation energy, $\bullet E^{prep}$, which corresponds to the energy necessary to promote the fragments from their equilibrium geometry and electronic ground state to the geometry and electronic state that they acquire in the complex geometry. With this approach, the bond dissociation energy can be estimated according to Eq.(8). Therefore, in this study the fragments that have already acquired their geometries in the complexes are taken as the reference for the interaction energy. The preparation energy, zero point energy and thermal energy are not included in the analysis.

$$-De = \Delta E^{prep} + \Delta E^{int} \quad (8)$$

According to the Su-Li EDA, the total interaction energy ΔE^{int} values for the $[NO]^+[Ru(NO_2)(bpy)_2]^+$ and $[NO]^+\leftrightarrow[Ru(ONO)(bpy)_2]^+$ interactions in **1a** and **3aZ** are considerably higher (-83.0 kcal mol^{-1} and -89.7 kcal mol^{-1}, respectively) than that for the $[ON]^+\leftrightarrow[Ru(ONO)(bpy)_2]^+$ interaction in complex **2aZ** (-39.4 kcal mol^{-1}). It is important to note that such interactions are modulated by the orbital term, ΔE^{pol}, that is, by the π-back-donation Ru→NO and Ru→ON in the $\{RuNO\}^6$ and $\{RuON\}^6$ cores, since the electrostatic interactions are repulsive in these cases, presenting positive ΔE^{ele} values, which are higher in **1a** and **3aZ** than in **2aZ**, in agreement with the calculated atomic charge distributions (Table S2). The ΔE^{pol} values obtained are in close agreement with the QTAIM

results, as previously described. Since the most important contribution in such interactions is that of the polarization component, it is also expected that the contribution of both the electron repulsion, ΔE^{rep}, and electron exchange, ΔE^{ex}, is significant. It is also important to note the very minor, although non-negligible, role of the dispersion contribution, ΔE^{disp}, in the $\{RuNO\}^6$ and $\{RuON\}^6$ interactions in comparison with ΔE^{pol} (Table 2).

Nitro↔nitrito isomerism of $\{RuNO\}^6$ cores.

Table 2 shows that the total interaction energy ΔE^{int} values are generally more negative for the nitro and nitrito groups than for the nitrosyl and isonitrosyl for complexes **1a**, **2a** and **3a**, independent of the nitrito configuration (Z or U). In the former case, the electrostatic energy ΔE^{ele} is the major term, modulating the interaction. The nitro interaction energy is only slightly greater than that of the nitrito (difference of 5.2 kcal mol^{-1}). In this regard, it is not only the electrostatic component that stabilizes $[NO_2]^- \leftrightarrow [Ru(NO)(bpy)_2]^+$ and $[ONO]^- \leftrightarrow [Ru(NO)(bpy)_2]$ but also the exchange, polarization and dispersion components. In fact, the higher value for the electrostatic energy reflects the Coulomb stabilizations of the nitrito interaction with the positively-charged metallic fragments.

Table 2. Su-Li EDA analysis results for the ruthenium nitrosyl bipyridine complexes before reduction in the ground and metastable states at the M06/Def2-SVP level of theory, where the components (in kcal mol^{-1}) are represented as follows, ΔE^{ele}=electrostatic energy, ΔE^{ex}=exchange energy, ΔE^{rep}=repulsion energy, ΔE^{pol}=polarization energy, ΔE^{disp}=dispersion energy and ΔE^{int}=total interaction energy.

Interactions	ΔE^{int}	ΔE^{ele}	ΔE^{rep}	ΔE^{ex}	ΔE^{pol}	ΔE^{disp}
1a						
$[NO]^+ \leftrightarrow [Ru(NO_2)(bpy)_2]^+$	-83.0	50.0	227.6	-48.6	-279.7	-32.2
$[NO_2]^- \leftrightarrow [Ru(NO)(bpy)_2]^{3+}$	-323.9	-281.6	142.1	-22.4	-119.0	-43.0
2a(Z)						
$[ON]^+ \leftrightarrow [Ru(ONO)(bpy)_2]^+$	-39.4	57.6	142.2	-22.0	-185.7	-31.5
$[ONO]^- \leftrightarrow [Ru(NO)(bpy)_2]^{3+}$	-329.0	-286.1	154.1	-27.7	-130.2	-39.1
2a(U)						
$[ON]^+ \leftrightarrow [Ru(ONO)(bpy)_2]^+$	-37.2	51.1	133.4	-18.2	-169.9	-33.6
$[ONO]^- \leftrightarrow [Ru(NO)(bpy)_2]^{3+}$	-316.7	-275.1	127.7	-15.9	-111.0	-42.4
3a(Z)						
$[NO]^+ \leftrightarrow [Ru(ONO)(bpy)_2]^+$	-89.7	49.5	224.6	-46.7	-283.0	-34.1
$[ONO]- \leftrightarrow [Ru(NO)(bpy)_2]^{3+}$	-329.0	-286.1	154.1	-27.7	-130.2	-39.1
3a(U)						
$[NO]^+ \leftrightarrow [Ru(ONO)(bpy)_2]^+$	-87.4	39.2	216.3	-43.0	-263.9	-36.0
$[ONO]- \leftrightarrow [Ru(NO)(bpy)_2]^{3+}$	-323.8	-277.1	134.2	-18.4	-119.7	-42.8

At this point it is important to mention how the magnitude of the Ru–NO, Ru–ON, Ru–NO_2 and Ru–ONO interactions is related to the total electronic energy and consequently the structural stability (Figure 4). The relative magnitude of the total interaction energy, ΔE, for different binding modes of the NO and NO_2^- groups for complexes **1a**, **2aZ**, **2aU**, **3aZ**, and **3aU** obtained from the Su-Li EDA analysis allows correlations with the relative structural stability (Figure 5) to be identified. The energy profile obtained with the total bonding energy is very similar to that obtained with the relative energy (Figure 4), indicating that stronger interactions lead to greater stability (Figure 4). Also, some differences are clearly observed. For instance, the U-forms of nitrito-ligand isomers (**2aU** and **3aU**) are slightly more stable than the Z forms (**2aZ** and **3aZ**). However, the Ru–NO, Ru–ON, Ru–NO_2 and Ru–ONO interaction energies, ΔE, are more stable in **2aZ** and **3aZ** than in **2aU** and **3aU**. In fact, the total ΔE values for complexes **1a** (ΔE^{int} = - 406.8 kcal mol^{-1}) and **3aZ** (ΔE^{int} = - 418.7 kcal mol^{-1}) compared to **2aZ** (ΔE^{int} = - 368.4 kcal mol^{-1}) (Table 2) suggest that **1a** and **3aZ** should be more stable than **2aZ** and that **3aZ** is expected to be the most stable form. In addition, the small difference in the ΔE values for **3a** and **1a** suggests that there should be a small difference in their stabilities. These results not only agree qualitatively with the calculated energy levels reported by Coppens and coworkers, in which the nitrosyl-nitrito form was energetically more stable (by ~ 1 kcal mol^{-1}) than the nitrosyl-nitro form, but also with the known synthetic methods which allow the preparation of both isomers.[49,50,53]

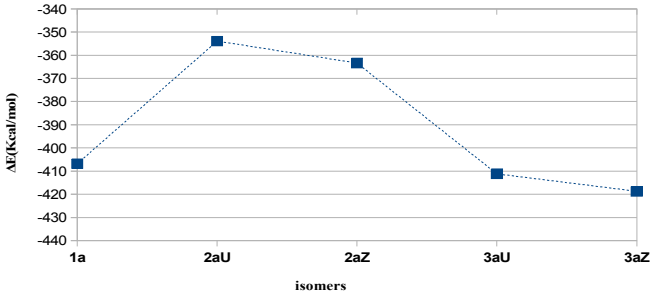

Fig. 5. Total interaction energy, ΔE, calculated as the sum of the individual ΔE^{int} values for each isomer, as compiled in Table 2.

Nitrosyl isomerism of {RuNO}^{7} cores.

The Su-Li EDA was also carried out for the reduced complexes, **1b-3b**, considering $[NO]^0 \leftrightarrow [Ru(NO_2)(bpy)_2]^+$, $[NO_2]^- \leftrightarrow [Ru(NO)(bpy)_2]^+$, $[ON]^0 \leftrightarrow [Ru(ONO)(bpy)_2]^+$, $[ONO]^- \leftrightarrow [Ru(ON)(bpy)_2]^+$, $[NO]^0 \leftrightarrow [Ru(ONO)(bpy)_2]^+$, and $[ONO]^- \leftrightarrow [Ru(NO)(bpy)_2]^+$ as interacting fragments (Table 3).

The monoelectronic reduction was modeled through the addition of one electron to NO π* orbital which has a major contribution to the LUMO orbital of $[Ru(NO)(NO_2)(bpy)_2]^{2+}$along with some contribution from the Ru d_{xy} atomic orbital. Upon reduction, a weakening of the Ru–NO π-bonding is expected (Figure 1, Table S1). Therefore, the Ru−NO bond weakening should be reflected in the magnitude of the total interaction energy, ΔE^{int}, in Su-Li EDA analysis. Indeed, the ΔE^{int} values are around 41% lower for **1b** and **3b** (-83.0 kcal mol^{-1} and -53.2 kcal mol^{-1}, respectively) when compared with the isomers **1a** and **3a** and around 46% lower for **2b** (-21.4 kcal mol^{-1}) when compared with **2a** (Table 2). As also observed for the {RuNO}^{6} species, for the {RuNO}^{7} species in the reduced complexes **1b** and **3b** the total interaction energy was greater than that observed for this **2b**, which implies that the $[NO]^0 \leftrightarrow [Ru(NO_2)(bpy)_2]^+$ and $[NO]^0 \leftrightarrow [Ru(ONO)(bpy)_2]^+$ interactions are stronger than the $[ON]^0 \leftrightarrow [Ru(ONO)(bpy)_2]^+$ interaction. The magnitude of these interactions is affected not only by the polarization, ΔE^{pol}, but also the electrostatic, ΔE^{ele}, component. After the monoelectronic reduction, the polarization between the interacting fragments is reduced, as shown by the magnitude of the polarization terms (ranging from -45.4 to -145.1 kcal mol^{-1}), which are in agreement with the decrease in the polarization coefficients and with the reduced charge of the NO group observed in the NBO analysis.

After the monoelectronic reduction complex **2b** has the lowest value for the polarization energy (-45.4 kcal mol^{-1}), which implies a weakening of the $[ON]^0 \leftrightarrow [Ru(ONO)(bpy)_2]^+$ interaction in **2b**. Table 3, shows that the electrostatic contribution to the total interaction energy is smaller than that of the polarization energy, although the magnitudes of these contributions are larger than those of the exchange and dispersion contributions, which range from -9.5 to -55.0 kcal mol^{-1} for ΔE^{ex} and -33.3 to -38.3 kcal mol^{-1} for ΔE^{disp}.

However, for complex **2b** the contribution of the dispersion energy (-33.3 kcal mol^{-1}) is more significant than that of the electrostatic energy (-26.6 kcal mol^{-1}). For all complexes, only the repulsion destabilizes the nitrosyl interaction with the metallic fragment. However, the polarization is still the major contribution in these interactions.

The repulsion term, ΔE^{rep}, for {RuNO}^{7} complexes than that for {RuNO}^{6}, despite the additional electronic repulsion, with values ranging from 93.5 kcal mol^{-1} to 233.3 kcal mol^{-1}. Although complex **2b** presents the lowest repulsion energy (93.5 kcal mol^{-1}) it was observed that the $[ON]^0 \leftrightarrow [Ru(ONO)(bpy)_2]^+$ interaction continues to be the less favorable due to the small contribution from the electrostatic and dispersion components. Considering the magnitude of the total interaction energy, ΔE^{int}, for the {RuNO}$^{6/7}$ cores, complex **2b**, *cis*-$[Ru(ON)(ONO)(bpy)_2]^+$, is more likely to release NO, through a photochemical process, when compared to complexes **1b** and **3b**.

Nitro↔nitrito isomerism of {RuNO}^{7} cores.

According to Table 3, the interaction of NO_2^- or ONO^- with reduced fragments is weaker than with non-reduced ones. This can be observed from the magnitude of the total interaction energy $\bullet E^{int}$, which is smaller for isomers **1b-3b**, (-220.7 to -223.2 kcal mol^{-1}) than for isomers **1a-3a** (-323.0 to -329.0 kcal mol^{-1}). Although the total interaction energies, ΔE^{int}, have similar values, the contributions of each component are different. After reduction, the magnitude of the electrostatic term (ΔE^{ele}) decreases while the repulsion term (ΔE^{rep}) increases. This repulsion effect is more pronounced for **1b** with the NO_2^- group (190.7 kcal mol^{-1}) than **2b** and **3b** with the ONO^- group (133.6 kcal mol^{-1} and 165.2 kcal mol^{-1}, respectively). These results may be rationalized as an effect of the decrease in Ru–NO π-back-donation which, in turn, increases the electron density in the metal center. As shown in Table 3, for complex **1b**, for the $[NO_2]^- \leftrightarrow [Ru(NO)(bpy)_2]^{2+}$ interaction, an increase in the magnitude of the polarization component, $\bullet E^{pol}$ (-113.7 kcal mol^{-1}) was observed. On the other hand, there is a decrease in this component for complexes **2b** (-99.9 kcal mol^{-1}) and **3b** (-111.1 kcal mol^{-1}). As this term is a direct measure of the charge transfer, after reduction the nitro form continues to contribute more to the charge transfer than the nitrito form. The results also show that the reduction of the NO group does not affect significantly the $[NO_2]^- \leftrightarrow [Ru(NO)(bpy)_2]^{2+}$ and $[ONO]^- \leftrightarrow [Ru(ON/NO)(bpy)_2]^{2+}$ interactions.

Table 3. Su-Li EDA analysis of ruthenium nitrosyl bipyridine complexes after reduction in the ground and metastable states at the M06/Def2-SVP level of theory, where the components (in kcal mol^{-1}) are represented as follows: ΔE^{ele}=electrostatic energy, ΔE^{ex}=exchange energy, ΔE^{rep}=repulsion energy, ΔE^{pol}=polarization energy, ΔE^{disp}=dispersion energy and ΔE^{int}=total interaction energy.

Interactions	ΔE^{int}	ΔE^{ele}	ΔE^{rep}	ΔE^{ex}	ΔE^{pol}	ΔE^{disp}
1b						
$[NO]^0 \leftrightarrow [Ru(NO_2)(bpy)_2]^+$	-50.3	-58.7	233.3	-55.0	-132.8	-37.1
$[NO_2]^- \leftrightarrow [Ru(NO)(bpy)_2]^{2+}$	-220.5	-214.6	190.7	-41.0	-113.7	-41.7
2b						
$[ON]^0 \leftrightarrow [Ru(ONO)(bpy)_2]^+$	-21.4	-26.6	93.5	-9.5	-45.4	-33.3
$[ONO]^- \leftrightarrow [Ru(ON)(bpy)_2]^{2+}$	-223.2	-197.2	133.6	-22.4	-99.9	-36.6
3b						

$[NO]^0 \leftrightarrow [Ru(ONO)(bpy)_2]^+$	-53.2	-48.4	231.7	-53.2	-145.1	-38.2
$[ONO]^- \leftrightarrow [Ru(NO)(bpy)_2]^{2+}$	-220.7	-203.3	165.2	-34.3	-111.1	-37.2

Summary and Conclusions

The nature of Ru–NO^+, Ru–ON^+, Ru–NO_2^-, and Ru–ONO bonding was investigated applying Su-Li EDA, prior to and after monoelectronic reduction. The calculated bonding strength values presented excellent agreement with the calculated energy levels reported by Coppens and coworkers, and indicated that the isomers **3a** and **1a** are more stable than **2a**. According to the Su-Li EDA analysis, the nitrito interactions with the ruthenium center are stronger than the nitrosyl interactions, with the electrostatic and polarization being those that modulate the magnitude of these interactions. The Su-Li EDA also indicated that the nitrosyl group interactions with the ruthenium center are stronger than those of isonitrosyl and that these interactions become weaker after the reduction. On the other hand, the nitro and nitrito interactions are similar and become weaker after the reduction. Additionally, and in agreement with previous studies, the results of the Su-Li EDA suggest that **2a**, *cis*-$[Ru(ON)(ONO)(bpy)_2]^{2+}$, is the most energetic state with the weakest Ru−ON and Ru−ONO interactions and also that this complex should release NO more easily when compared to **1a** and **3a**.

The structures observed for *cis*-$[Ru(NO)(NO_2)(bpy)_2]^{2+}$ in the GS and MS states prior to and after one-electron reduction characterize the nitrosonium and nitrosyl nature, respectively, of the NO group. The Ru−NO bond in $\{RuNO\}^6$ is linear for (isomers **1a-3a**) and bent for $\{RuNO\}^7$ (isomers **1b-3b)**. The latter complexes also showed an increase in the Ru−NO and N−O bond lengths and a decrease in the ν(NO) vibrational frequencies regarding the reduced forms. The structural *trans*-effect of NO is greater than that of NO_2^- and both are influenced by the coordination modes of these groups and one-electron reduction. The lowest STE value was observed for *cis*-$[Ru(ON)(ONO)(bpy)_2]^{+/0}$.

The topological analysis confirmed the covalent character of the N−O and O−N bonds, which was more pronounced for the complexes in the GS and MS1 at 200 K. The Ru−NO and Ru−ON interactions have a closed-shell character and in the MS1 at 90 K the weakest interaction was observed due to the greater electron delocalization over the isonitrosyl group. The QTAIM analysis results confirmed those of the Su-Li EDA, that is, the nitrito and nitro coordinated environments have few differences. Although the nitro bonds N(2)−O(2) and N(2)−O(3) are electronically similar, due to the resonance effect, for nitrito groups these bonds are very different. Through NBO analysis it was also confirmed that Ru−ON in **2a** isomers are the weakest bonds, with a stronger donor-acceptor nature, rather than the single bond character present by the **1a** and **3a** isomers. The electronic population over the isonitrosyl group in **2a** also confirms the electron delocalization and the lower repulsion interaction of Ru□ON as indicated by the Su-Li EDA analysis.

Acknowledgments

The authors thank FAPESC, FAPESB and CNPq for the financial support.

References

1. J. A. McCleverty*, Chem. Rev.,* 2004*,* **104***,* 403.
2. E. Tfouni, D. R. Truzzi, A. Tavares, A. J. Gomes, L. E. Figueiredo and D. W. Franco, *Nitric Oxide*, 2012, **26**, 38.
3. A. D. Ostrowski, P. C. Ford, *Dalton Trans.*, 2009, **48**, 10660.
4. M. J. Rose and P. K. Mascharak, *Coord. Chem. Rev.*, 2008, **252**, 2093.
5. M. G. Sauaia, F. S. Oliveira, A. C. Tedesco and R. S. da Silva, *Inorg. Chim. Acta*, 2003, **355**, 191.
6. P. De, T. K. Mondal, S. M. Mobin and G. K. Lahiri, *Inorg. Chim. Acta,* 2011*,* **372**, 250.
7. P. C. Ford, L. E. Laverman, *Coord. Chem. Rev.*, 2005, **249**, 391.
8. B. Machura, *Coord. Chem. Rev.,* 2005, **249**, 2277.
9. A. Klein, I. von Mering, A. Uthe, K. Butsch, D. Schaniel, N. Mockus and T. Woike*, Polyhedron,* 2010*,* **29**, 2553.
10. P. C. Ford, J. Bourassa, K. Miranda, B. Lee, I. Lokorvic, S. Boggs, S. Kudo and L. E. Laverman, *Coord. Chem. Rev.,* 1998, **171**, 185.
11. C. de La Cruz and N. A. Sheppard, *Spectrochim. Acta, Part A*, 2011, **78**, 7.
12. J. B. Raynor, *Inorg. Chim. Acta*, 1972, **6**, 347.
13. M. J. Clarke, *Coord. Chem. Rev.*, 2003, **236**, 209.
14. Inorg. Chem.: Forum in Nitric Oxide, 2010, **49**, 6223.
15. J. H. Enemark and R. D. Feltham, *Coord. Chem. Rev*., 1974, **13**, 339.
16. P. Coopens, I. Novozhilova and A. Kovalevsky, *Chem. Rev*., 2002, **102**, 861.
17. T. E. Bitterwolf, *Coord. Chem. Rev.*, 2006, **250**, 1196.
18. A. C. Merkle and N. Lehnert, *Inorg. Chem.*, 2009, **48**, 11504.
19. E. I. Tocheva, F. I. Rosell, A. G. Mauk and M. E. Murphy, *Science*, 2004, **304**, 867.
20. C. Nathan, *FASEB J*., 1992, **6**, 3051.
21. J. Marin and C. F. Sanchez-Ferrer, *Gen. Pharmacol.*, 1990, **21**, 575.
22. L. J. Ignarro, Nitric Oxide: Biology and Pathobiology, 2000, 1ed, Academic Press, San Diego.
23. T. J. Anderson, I. T. Meredith, P. Ganz, A. P. Selwyn and A. C. Yeung, *J. Am. Coll. Cardiol.*, 1994, **24**, 555.
24. S. Moncada, R. M. J. Palmer and E. A. Higgs, *Pharmacol. Rev.,* 1991, **43**, 109.
25. D. A. Wink and J. B. Mitchell, *Free Radic. Biol. Med.*, 1998, **25**, 434.
26. A. R. Butler and I. L. Megson, *Chem. Rev.*, 2002, **102**, 1155.
27. A. L. Speelman and N. Lehnert, *Angew. Chem., Int. Ed*., 2013, **52**, 12283.
28. R. Foresti, R. Motterlini, *Free Rad. Res.*, 1999, **31**, 459.
29. N. Xu, J. Yi, G. B. Richter-Addo, *Inorg. Chem*., 2010, **49**, 6253.
30. N. Xu, L. E. Goodrich, N. Lehnert, D. R. Powell and G. B. Richter-Addo, *Angew. Chem., Int. Ed.*, 2013, **52**, 3896.
31. L. E. Goodrich, F. Paulat, V. K. K. Praneeth and N. Lehnert*, Inorg. Chem.*, 2010, **49**, 6293.
32. E. Tfouni, F. G. Doro, L. E. Figueiredo, J. C. M. Pereira, G. Metzker and D. W. Franco, *Curr. Med. Chem.*, 2010, **17**, 3643.
33. E. Tfouni, M. Krieger, B. R. McGarvey and D. W. Franco, *Coord. Chem. Rev*., 2003, **236**, 57.
34. Z. Carneiro, J. C. B. de Morais, F. P. Rodrigues, R. G. de Lima, C. Curti, Z. N. da Rocha, M. Paulo, L. M. Bendhack, A. C. Tedesco, A. L. B. Formiga and R. S. da Silva, *J. Inorg. Biochem.*, 2011, **105**, 1035.
35. A. L. Noffke, M. Bongartz, W. Wätjen, P. Böhler, B. Spingler and P. C. Kunz *J. Organomet. Chem.,* 2011*,* **696**, 1096.
36. M. Matiková-Maľarová, R. Novotná and Z. Trávníček, *J. Mol. Struct.***,** 2010, **977**, 203.
37. B. R. McGarvey, A. A. Ferro, E. Tfouni, C. W. B. Bezerra, I. Bagatin and D. W. Franco, *Inorg. Chem.*, 2000, **39**, 3577.

38. V. K. K. Praneeth, F. Paulat, T. C. Berto, S. D. George, C. Nather, C. D. Sulok and N. Lehnert, *J. Am. Chem. Soc.*, 2008, **130**, 15288.
39. J. B. Godwin and T. J. Meyer, *Inorg. Chem.*, 1971, **10**, 471.
40. V. Togniolo, R. S. da Silva and A. C. Tedesco, *Inorg. Chim. Acta*, 2001, **316**, 7.
41. C. N. Lunardi, A. L. Cacciari, R. S. da Silva and L. M. Bendhack, *Nitric Oxide*, 2006, **15**, 252.
42. A. C. Pereira, P. C. Ford, R. S. da Silva and L. M. Bendhack, *Nitric Oxide*, 2011, **24**, 192.
43. D. V. Fomitchev, P. Coppens, T. Li, K. A. Bagley, L. Chen and G. B. Richter-Addo, *Chem. Commun.*, 1999, 2013.
44. O. V. Sizova, V. V. Sizov and V. I. Baranovski, *J. Mol. Struct.: THEOCHEM***,** 2004, **683**, 97.
45. H. Giglmeier, T. Kerscher, P. Klüfers, S. Schaniel and T. Woike, *Dalton Trans.,* 2009, 9113.
46. T. E. Bitterwolf, *Inorg. Chem.*, 2008, **11**, 772.
47. D. V. Fomitchev, I. Novozhilova and P. Coppens, *Tetrahedron*, 2000, **56**, 6813.
48. O. Lyubimova, O. V. Sizova, C. Loschen and G. Frenking, *J. Mol. Struct.*, 2008**, 865**, 28.
49. D. Ooyama, N. Nagao, H. Nagao, Y. Miura, A. Hasegawa, K. Ando, F. S. Howell, M. Mukaida and K. Tanaka, *Inorg. Chem.*, 1995, **34**, 6024.
50. D. Ooyama, Y. Miura, Y. Kanazawa, F. S. Howell, N. Nagao, M. Mukaida, H. Nagao and K. Tanaka, *Inorg. Chim. Acta,* 1995, **237**, 47.
51. O. A. Ileperuma and R. D. Feltham, *J. Am. Chem. Soc.*, 1976, **98**, 6039.
52. J. L. Hubbard, C. R. Zoch and W. L. Elcesser, *Inorg. Chem.*, 1993**, 32**, 333.
53. Y. Kovalevsky, G. King, K. A. Bagley and P. Coppens, *Chem. Eur. J.* 2005, **11**, 7254.
54. B. Delley, J. Schefer and T. Woike, *J. Chem. Phys*, 1997, **107**, 10067.
55. C. D. Kim, I. Novozhilova, M. S. Goodman, K. A. Bagley and P. Coppens, *Inorg. Chem.*, 2000, **39**, 5791.
56. S. I. Gorelsky, S. C. da Silva, A. B. P. Lever and D. W. Franco, *Inorg. Chim. Acta*, 2000, **300-302**, 698.
57. S. I. Gorelsky and A. B. P. Lever, *Int. J. Quantum Chem.*, 2000, **80,** 636.
58. P. Boulet, M. Buchs, H. Chermette, C. Daul, F. Gilardoni, F. Rogemond, C. W. Schläpfer and J. Weber, *J. Phys. Chem. A*, 2001, **105**, 8991.
59. P. Boulet, M. Buchs, H. Chermette, C. Daul, F. Gilardoni, F. Rogemond, C. W. Schläpfer and J. Weber, *J. Phys. Chem. A*, 2001, **105**, 8999.
60. O. V. Sizova, N. V. Ivanova, V .V. Sizov and A. B. Nikolskii, *Russ. J. Gen. Chem.*, 2004, **74**, 481.
61. O. V. Sizova, O. O. Lyubimova and V. V. Sizov, *J. Mol. Struct. THEOCHEM*, 2004, **712**, 33.
62. A. K. Das, B. Sarkar, C. Duboc, S. Strobel. J. Fiedler, S. Zális, G. K. Lahiri and W. Kaim, *Angew. Chem. Int. Ed.*, 2009, **48,** 4242.
63. P. De, B. Sarkar, S. Maji, A. K. Das, E. Bulak, S. M. Mobin, W. Kaim and G. K. Lahiri, *Eur. J. Inorg. Chem.*, **2009,** 2702.
64. N. Lehnert and W. R. Scheidt, *Inorg. Chem.,* 2010, **49**, 6223.
65. G. K. Lahiri and W. Kaim, *Dalton. Trans.*, 2010, **39**, 4471.
66. P. De, T. K. Mondal, S. M. Mobin, and G. K. Lahiri, *Inorg. Chim. Acta*, 2011, **372,** 250.
67. P. De, S. Maji, A. Chowdhury, S. M. Mobin, T. K. Mondal, A. Paraetzki and G. K. Lahiri, *Dalton. Trans.*, 2011, **40**, 12527.
68. A. D. Chowdhury, P. De, S. M. Mobin and G. K. Lahiri, *RSC Adv.*, 2012, **2,** 3437.
69. P. Su. and H. Li, *J. Chem. Phys.*, 2009, **131**, 014102.
70. R. F. W. Bader. *Atoms and Molecules-A Quantum Theory*, Claredon Press, Oxford, New York, 1994.
71. C. F. Matta, R. J. Boyd. *The Quantum Theory of Atoms in Molecules*, Wiley-VCH, Nova Scotia, 2007.
72. M. Rafat, M. Devereux and P. L. A. Popelier, *J. Mol. Graphics Modell.,* 2005, **24**, 111.
73. P. L. A. Popelier and G. Logothetis, *J. Organomet. Chem.,* 1998, **555**, 101.
74. P. L. A. Popelier, *Comput. Phys. Commun.*, 1998**, 108**, 180.
75. F. Weinhold and C. R. Landis**,** *Chem. Educ. Res. Pract. Eur.*, 2001, **2**, 91.
76. F. Neese, *WIREs Comput. Mol. Sci.*, 2012, **2**, 73.
77. M. W., Schmidt, K. K. Baldrige, J. A. Boatz, S. T. Elbert, M. S. Gordon, J. H. Jensen, S. Koseki, N. Matsunaga, K. A. Nguyen, S. J. Su, T. L. Windus, M. Dupuis and J. A. Montgomery, *J. Comput. Chem.*, 1993, **14**, 1347.
78. Gaussian 03, Revision D.01, M. J. Frisch, G. W. Trucks, H. B. Schlegel, G. E. Scuseria, M. A. Robb, J. R. Cheeseman, J. A. Montgomery, Jr., T. Vreven, K. N. Kudin, J. C. Burant, J. M. Millam, S. S. Iyengar, J. Tomasi,V. Barone, B. Mennucci, M. Cossi, G. Scalmani, N. Rega, G. A. Petersson, H. Nakatsuji, M. Hada, M. Ehara, K. Toyota, R. Fukuda, J. Hasegawa, M. Ishida, T. Nakajima, Y. Honda, O. Kitao, H. Nakai, M. Klene, X. Li, J. E. Knox, H. P. Hratchian, J. B. Cross,V. Bakken, C. Adamo, J. Jaramillo, R. Gomperts, R. E. Stratmann, O. Yazyev, A. J. Austin, R. Cammi, C. Pomelli, J. W. Ochterski, P. Y. Ayala, K. Morokuma, G. A. Voth, P. Salvador, J. J. Dannenberg, V. G. Zakrzewski, S. Dapprich, A. D. Daniels, M. C. Strain, O. Farkas, D. K. Malick, A. D. Rabuck, K. Raghavachari, J. B. Foresman, J. V. Ortiz, Q. Cui, A. G. Baboul, S. Clifford, J. Cioslowski, B. B. Stefanov, G. Liu, A. Liashenko, P. Piskorz, I. Komaromi, R. L. Martin, D. J. Fox, T. Keith, M. A. Al-Laham, C. Y. Peng, A. Nanayakkara, M. Challacombe, P. M. W. Gill, B. Johnson, W. Chen, M. W. Wong, C. Gonzalez, and J. A. Pople, Gaussian, Inc., Wallingford CT, 2004.
79. A. D. Becke, *Phys. Rev. A: At., Mol., Opt. Phys.,* 1988, **38**, 3098.
80. J. P. Perdew, *Phys. Rev. B*, 1986, **33**, 8822.
81. A. Becke and K. E. Edgecombe, *J. Chem. Phys.*, 1990, **92**, 5397.
82. D. A. Pantazis, X. Y. Chen, C. R. Landis and F. Neese*, J. Chem. Theory Comput.*, 2008**, 4**, 908.
83. D. Andrae, U. Haeussermann, M. Dolg, H. Stoll and H. Preuss*, Theor. Chim. Acta,* 1990*,* **77**, 123.
84. F. Weigend, *Phys. Chem. Chem. Phys.,* 2006, **8**, 1057.
85. E. van Lenthe, E. J. Baerends and J. G. Snijders*, J. Chem. Phys.,* 1993, **99**, 4597.
86. E. van Lenthe, E. J. Baerends and J. G. Snijders, *J. Chem. Phys.*, 1996, **105**, 6505.
87. K. Morokuma, *J. Chem. Phys.*, 1971, **55**, 1236.
88. K. Morokuma, *Acc. Chem. Res.*, 1977, **10**, 294.
89. T. Ziegler and A. Rauk, *Theor. Chim. Acta*, 1977, **46**, 1.
90. I. C. Hayes and A. J. Stone, *Molec. Phys.*, 1984, **53**, 83.
91. S. F. Boys and F. Bernardi, *Mol. Phys.*, 1970, **19**, 553.
92. Y. Zhao and D. G. Truhlar, *Theor. Chem. Acc.,* 2007*,* **120**, 215.
93. Y. Zhao and D. G. Truhlar, *Acc. Chem. Res.,* 2008, **41**, 157.
94. AIMAll (Version 12.11.09), T. A. Keith, TK Gristmill Software, Overland Park KS, USA, 2012 (aim.tkgristmill.com)
95. T. Lu and F. Chen, *J. Comp. Chem.,* 2012*,* **33**, 580.
96. A. C. Merkle, A. B. McQuarters and N. Lehnert, *Dalton. Trans.*, 2012, **41**, 8047.
97. G. F. Caramori and G. Frenking, *Organomettalics,* 2007, **26**, 5815.
98. G. F. Caramori, A. G. Kunitz, K. F. Andriani, F. G. Doro, G.

Frenking and E. Tfouni, *Dalton Trans.,* 2012, **41**, 7327.
99. N. Lehnert, J. T. Sage, N. Silvernail, W. R. Scheidt, E. E. Alp, W. Sturhahn and J. Zhao, *Inorg. Chem.*, 2010, **45**, 7197.
100. V. K. K. Praneeth, C. Nather, G. Peters and N. Lehnert, *Inorg. Chem.*, 2006, **45**, 2795.
101. G. R. Wyllie, C. E. Schulz and W. R. Scheidt, *Inorg. Chem.* 2003, **42**, 5722.
102. B. J. Coe and S. J. Glenwright, *Coord. Chem. Rev.*, 2000, **203**, 5.
103. N. Lehnert, U. Cornelissem, F. Neese, T. Ono, Y. Noguchi, K. Okamoto and K. Fujisawa, *Inorg. Chem.*, 2007, **46**, 3916.

Ru□NO and Ru□NO_2 Bonding Linkage Isomerism in *cis*-$[Ru(NO)(NO_2)(bpy)_2]^{2+/+}$ Complexes – A Theoretical Insight

Karla Furtado Andriani,*[a] Giovanni Finoto Caramori,[a] Fábio Gorzoni Doro[b,c] and Renato Luis Tame Parreira.[d]

[a]Departamento de Química, Universidade Federal de Santa Catarina, Campi Universitário Trindade, 88040-900 Florianópolis – SC, Brazil.
[b]Departamento de Química Geral e Inorgânica, Universidade Federal da Bahia – UFBA, Salvador – BA, Brazil.
[c]Departamento de Química, Faculdade de Filosofia, Ciências e Letras de Ribeirão Preto. Universidade de São Paulo – [d]FFCLRP, Ribeirão Preto – SP, Brazil. (present address)
Núcleo de Pesquisas em Ciências Exatas e Tecnológicas, Universidade de Franca – UNIFRAN, Franca – SP, Brazil.

Calculated energy profile (kcal mol^{-1}) for linkage isomers relative to the ground state structure (GS) **1a**, prior the monoelectronic reduction, at BP86/Def2-TZVPP level of theory. The energy levels are computed taking into account the changes in the nitrito-ligand configuration (U-form and Z-form).